Surface water quality in the Fen River Basin: 2016–2023 trends, the COVID-19 lockdown effects, and water governance implications

Linlin Li[1], Shaoyong Lu[1], Bingfen Cheng[2*], Yizhang Zhang[1], Zuqin Shi[1]

(1. State Key Laboratory of Environmental Criteria and Risk Assessment, State Environmental Protection Key Laboratory for Lake Pollution Control, National Engineering, Beijing, 100012, China; 2. College of Emergency Technology and Management, North China Institute of Science & Technology, Langfang, 065201, China.)

*Corresponding author: bingfenlove@126.com; stulilinlin@163.com

Abstract

This study examined water quality trends in the Fen River Basin from 2016 to 2023, utilizing data from seven monitoring stations. Advanced statistical methods, including the Daniel trend test, Seasonal and Trend decomposition using Loess (STL), grey correlation analysis, and Long Short-Term Memory (LSTM) neural networks, were employed to identify trends and key influencing factors. Over this period, the average Chemical Oxygen Demand (COD) and Ammonia Nitrogen (NH_4^+-N) concentrations across Fen River Basin were (25.3±17.3) $mg \cdot L^{-1}$ and (3.6±3.2) $mg \cdot L^{-1}$, respectively. Water quality improved significantly, transitioning from severe pollution in 2016 to mild pollution in 2023. The upstream consistently maintained higher quality, generally classified as Class I or II according to GB 3838-2002 standards, while the middle and lower reaches exhibited poorer conditions. The previously prevalent inferior Class V water quality has largely been eradicated. Key indicators such as COD and NH_4^+-N in the middle and lower reaches demonstrated statistically significant improvements at a 95% confidence level. However, reductions in NH_4^+-N concentrations were inconsistent in some upstream areas. These improvements are consistent with enhanced water source protection and stricter pollution control measures. Nonetheless, excessive pollutant discharge, particularly from domestic and industrial sources, continues to challenge the river's self-purification capacity, resulting in localized water quality fluctuations, which are most evident in the middle and lower reaches. Notably, a significant improvement in water quality was observed during the COVID-19 lockdown, attributed to reduced water usage across industrial, agricultural, and domestic sectors. This highlights the efficacy of emission reduction strategies and the potential for targeted management to achieve further gains. LSTM-based predictions suggest that COD concentrations in the middle and lower reaches will meet Class II surface water standards (15 mg/L) by the end of the 14th Five-Year Plan. However, NH_4^+-N concentrations are projected to exceed the Class II limit (0.5 mg/L) during dry seasons. Future efforts should concentrate on mitigating seasonal NH_4^+-N variations to sustain and enhance water quality improvements.

Key words: spatio-temporal variations; water quality; influencing factors; LSTM; Fen River

1 Introduction

Rivers serve as vital water resource transportation channels from land to lakes and oceans, fulfilling critical societal needs such as drinking water, irrigation, and hydropower generation (Grill et al., 2019). They support domestic, agricultural, and energy needs, playing a pivotal role in sustaining human society. However, rapid socio-economic development over recent decades have led to high-intensity human activities that have not only depleted significant water resources but also severely degraded water quality. This degradation has damaged river ecosystems and poses a serious threat to human water safety and the integrity of aquatic ecosystems (Chen et al., 2019；Xia et al., 2020). Recent studies have highlighted that the input of pollutants from rivers in China is significant. Pollutant loads include 2.8×10^7 tons of dissolved nitrogen, 3×10^6 tons of dissolved phosphorus (Chen et al., 2019), and nearly 2.5×104 tons of antibiotics (Zhang et al., 2015). In 2022, data from 3,629 monitoring stations across China showed that 87.9% of water quality assessments fell within Classes I to III, while only 0.7% were rated as Class V. Key pollution indicators included chemical oxygen demand (COD), total phosphorus (TP), and potassium permanganate index (CODMn) (Ministry of Ecology and Environment, 2023). This water pollution crisis is further compounded by an annual shortage of 40 billion tons of water in China (Tao and Xin, 2014).

Many studies have increasingly focused on the evolution of water quality in China's major rivers and the factors driving these changes, particularly in the seven key river systems that are vital to the nation's economy, ecology, and society. (Meng and Zhang,2023; Qiao et al.,2021; Huang et al.,2021). For instance, Zhang et al. (2020) identified COD, biochemical oxygen demand (BOD), and TP as the primary water pollution indicators in these river systems. Their study also noted significant improvements in China's Class V surface water between 2005 and 2017. To analyze the spatio-temporal variations in river water quality, researchers commonly employ statistical methods such as Mann Kendall test, Daniel trend test, cluster analysis, spatial interpolation, Spearman correlation analysis, and grey correlation analysis (Zhai et al.,2014； Huang et al.,2021). However, while these methods have provided valuable insights, the mechanisms underlying water quality evolution are complex and multifaceted (Venkatraman et al., 2025). Key influencing factors include both

human activities and natural conditions (Cheng et al., 2019). Despite significant progress in understanding these dynamics, a major limitation in current research is the lack of long-term observational data, which hinders the ability to fully grasp the long-term trends and causes of water quality fluctuations (Suresh et al., 2025). Furthermore, there is limited integration of manual and automatic monitoring data, which restricts comprehensive comparisons and analyses of river water quality evolution using advanced multiple spatio-temporal methods. Ongoing human activities have hindered further exploration of the natural and human factors driving water quality and their contributions. The COVID-19 pandemic, however, has provided an unprecedented opportunity to study the rapid improvement in water quality resulting from the reduction of human activities. During the lockdowns, decreased industrial production, transportation, and other human activities led to noticeable improvements in water quality, as documented in several studies (Kang et al., 2020; Deng and Peng, 2020; Le et al., 2020). This phenomenon has been observed globally, with notable examples including the canals of Venice (Saadat et al., 2020), the Yamuna River in India (Arif et al., 2020), and sections of the Yangtze River in China (Liu et al, 2022). Similarly, in the Fen River Basin, located in Shanxi Province, water quality has emerged as a critical concern. As the birthplace of the Three Jin Civilization, the Fen River Basin is densely populated and serves as the economic hub of Shanxi. (Gu et al., 2020). Despite severe surface water pollution and significant water shortages, the demand for water in urban, industrial, and agricultural sectors remains high. The quality of water in the Fen River directly impacts both resource utilization and sustainable economic development (Shanxi Provincial Bureau of Statistics, 2023). Consequently, water quality analysis and pollution control are central to the ecological and environmental protection strategy outlined in Shanxi Province's 14th Five-Year Plan.

To address these challenges, this study utilized manual and automatic water quality monitoring data collected from seven stations across the Fen River Basin, spanning the period from 2016 to 2023. A range of analytical methods—including Daniel trend analysis, STL trend decomposition, grey correlation degree, and long short-term memory (LSTM) neural network—was applied to comprehensively analyze water quality variations and identify key influencing factors. The goal is to provide technical support for pollution control measures and sustainable water management in

the Fen River Basin.

2 Materials and methods

2.1 Study area and observations

The Fen River, often referred to as the "mother river" of Shanxi, is the second-largest tributary of the Yellow River and plays a crucial role in the ecological security of the middle and lower reaches of the Yellow River. Originating from Ningwu County, the Fen River flows through six cities in Shanxi Province: Xinzhou, Taiyuan, Lvliang, Jinzhong, Linfen, and Yuncheng. It traverses the Jinzhong and Linfen basins, joined by more than ten tributaries along its 716 km length. With a drainage area of 39,721 km2, the Fen River accounts for approximately 25.5% of Shanxi Province's t total surface area (Figure.1). The river's upper reaches extend from its source to Shanglan Station in Taiyuan City, primarily flowing through mountainous areas. The middle section spans from Shanglan Station to Shitan in Hongdong County, passing through the Jinzhong Basin. The downstream section runs from Shitan to Huangkou. The Fen River Basin experiences a semi-arid to semi-humid continental monsoon climate, with an average annual precipitation of 504.8 mm, predominantly occurring between June and September. The basin's total water resources amount to 3.358 billion cubic meters, representing approximately 27.2% of Shanxi Province's total water resources (Shanxi Provincial Bureau of Statistics, 2023). Water quality monitoring data, including chemical oxygen demand (COD) and ammonia nitrogen (NH_4^+-N), were obtained from seven monitoring stations in the Fen River Basin between 2016 and 2023. These data were sourced from the Shanxi Provincial Ecological Environment Bureau's Surface Water Environmental Quality Report (https://sthjt.shanxi.gov.cn/shjzl/dbsszyb/, as shown in Fig.1). T The seven monitoring stations are located at Leiming Temple (LMS), Hexi Village (HXC), Fen Reservoir (FHSK), Shanglan (SL), Wangzhuang Bridge South (WZQN), Shangpingwang (SPW), and Miaoqian Village (MQC). Water quality indicators were manually monitored once per month, and the sampling, analysis, and evaluation were carried out in accordance with the "Surface Water Environmental Quality Standards" (GB3838-2002). In certain months, no measurements were available due to dehydration or icing. In addition to the manual monitoring data, automatic water quality monitoring data from five stations in the Fen River Basin were used for the period from 2020 to 2023. These data were sourced from the national real-time data

release system for surface water quality monitoring (http://106.37.208.243:8068/GJZ/Business/Publish/Main.html). The five monitoring stations are located at Hexi Village (HXC), Fen Reservoir (FHSK), Shanglan (SL), Wangzhuang Bridge South (WZQN), and Shangpingwang (SPW). The main water quality indicators monitored include dissolved oxygen (DO), chemical oxygen demand (CODMn), ammonia nitrogen (NH4+-N), total phosphorus (TP), and water turbidity (TUR). Monitoring was conducted every four hours, with readings taken at 4:00, 8:00, 12:00, 16:00, and 20:00.

Data on annual precipitation and surface water resources across various cities in the Fen River Basin from 2016 to 2023 were sourced from the Water Resources Bulletin of Shanxi Province (http://slt.shanxi.gov.cn/zncs/szyc/szygb/). Discharge data for sewage and wastewater from various cities in the Fen River Basin, covering the period from 2016 to 2022, were obtained from the Statistical Yearbook of Urban and Rural Construction (http://www.mohurd.gov.cn/xytj/tjzljsxytjgb/jstjnj/). Additionally, GDP, population, and other statistical data from the cities within the Fen River Basin from 2016 to 2023 were sourced from the Shanxi Provincial Statistical Yearbook (http://www.shanxi.gov.cn/sj/tjnj/).

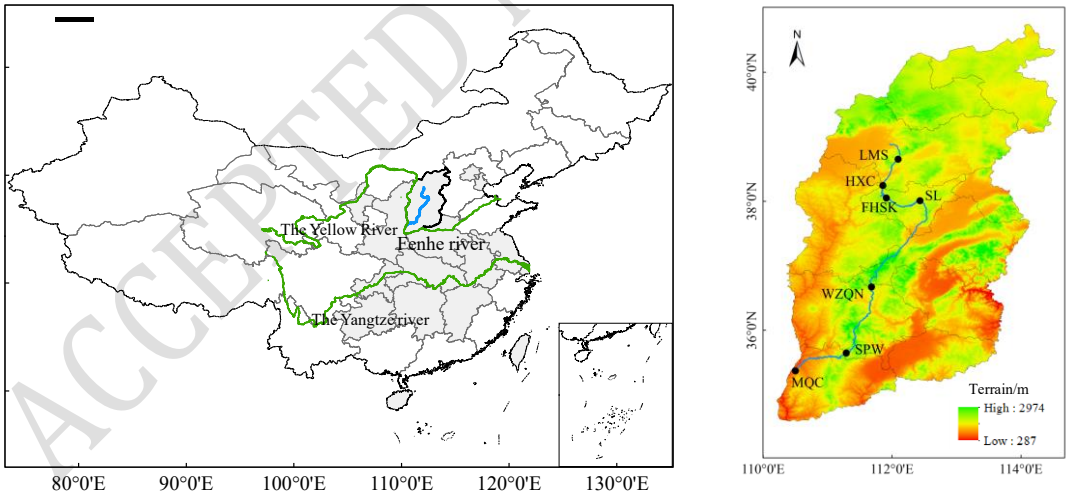

(a) Fenhe river basin (b) Distribution of observation stations

Fig.1 Geographical location and distribution of monitoring station

2.2 Daniel Trend Test

To analyze the trends of the water quality indicators, the Daniel trend test is applied in this study. Also known as Spearman's rank correlation coefficient test (Spearman,1904), this method is used to assess the correlation between two sets of variables (Daniel et al.,1990). Spearman's rank correlation coefficient is a

non-parametric statistical measure, meaning it does not rely on the distribution of data. The principle of the test involves assigning ranks to two variables, X and Y, where X_i and Y_i represent the ranks of the variables, respectively. The correlation between these two variables is then calculated using the following equation 2.1.

$$r_s = 1 - \left(6\sum_{i=1}^{n} (x_i - y_i)^2 \right) / \left(n^3 - n \right) \quad \text{(EQ2.1)}$$

In equation 2.1, r_s presents the Spearman rank correlation coefficient; X_i and Y_i are the ranks of the respective variables, and N is the number of observations. If $|r_s|$ ≥WP and Rs is positive, the data represents a significant upward trend; when $|r_s|$ ≥WP and r_s is negative, the data indicates a significant downward trend. Daniel Trend Test is suitable for the correlation test of a single factor with a small sample size, and it is concise with high accuracy. However, it performs poorly in the trend test of long-term sequences.

2.3 STL decomposition method

The STL (A Seasonal and Trend decomposition using Loss) method, introduced by Cleveland et al. (1979), is used for time series decomposition. It is based on LOESS (Locally Weighted Scatterplot Smoothing), a non-parametric regression technique that assigns varying weights to data points based on their proximity, allowing for flexible smoothing of non-linear data (Cleveland and Devlin, 1988). Each recursive process of the STL method requires three LOESS and one sliding average to be performed separately. In the STL method, the original data Y_t is decomposed into three components: trend ($Trend_t$), seasonal ($Seasonal_t$), and residual ($Residual_t$):

$$Y_t = Trend_t + Seasonal_t + Residual_t \quad \text{(EQ 2.2)}$$

The trend component represents the long-term, low-frequency behavior of the data under specific climatic conditions, while the seasonal term captures periodic fluctuations. STL has been widely applied in various fields such as economics, environmental science, and water quality analysis (Silawan et al., 2008). And it can handle seasonal components of different lengths and periods, and is applicable to time series data of various seasonal patterns.

2.4 LSTM method for prediction

Long Short-Term Memory (LSTM) networks, an improved version of Recurrent

Neural Networks (RNN), were introduced by Hochreiter and Schmidhuber (1997) to address the vanishing gradient problem. In this study, the LSTM network is utilized for water quality prediction, as it excels in modeling temporal dependencies in time series data.

Unlike traditional RNNs, which rely on a single neuron with a tanh activation function, LSTM introduces a "gate" mechanism that regulates the flow of information through the network's cell state. (Gers et al., 2003). Specifically, LSTM contains three gates: the input gate, the output gate, and the forget gate. These gates control the information added to or removed from the cell state, which allows the network to retain long-term dependencies.

The LSTM model used in this study has 200 hidden layer nodes, a sliding window size of 3 months, and a total of 12 iterations. For prediction, the fourth month's water quality is forecasted based on data from the first three months, the fifth month based on data from months 2−4, and so on.

The corresponding LSTM equations are as follows

$$f_t = \sigma(W_f[h_{t-1}, x_t] + b_f) \quad \text{(EQ2.3)}$$

$$i_t = \sigma(W_i[h_{t-1}, x_t] + b_i) \quad \text{(EQ 2.4)}$$

$$\overline{C_t} = \tanh(W_c[h_{t-1}, x_t] + b_c) \quad \text{(EQ2.5)}$$

$$C_t = f_t C_{t-1} + i_t \overline{C_t} \quad \text{(EQ2.6)}$$

$$o_t = \sigma(W_o \cdot [h_{t-1}, x_t] + b_o) \quad \text{(EQ2.7)}$$

$$h_t = o_t \tanh(C_t) \quad \text{(EQ2.8)}$$

In these equations, x_t is the input at time t; W is the weight matrix; b is the bias matrix; and $\overline{C_t}$ is the cell state at time t; C_t is the updated value at time t; h_t and h_{t-1} represent the outputs at times t and $t-1$, respectively. It is relatively insufficient in processing extremely long sequence data, and the training process has high computational complexity and takes a lot of time.

3 Results and Discussions

3.1 Temporal variations in water quality

As shown in **Fig.2**, during the sampling period from 2016 to 2023, the average concentrations of COD and NH_4^+-N at four monitoring sites in the upper reaches of the Fen River Basin were (5.6 ± 3.3) $mg \cdot L^{-1}$ and (0.12±0.09) $mg \cdot L^{-1}$, respectively. In contrast, the average COD and NH_4^+-N concentrations at three monitoring points in the middle and lower reaches were (25.3±17.3) $mg \cdot L^{-1}$ and (3.6 ± 3.2) $mg \cdot L^{-1}$, respectively. These results highlight the poor water quality in the middle and lower reaches compared to the upstream sections. At the WZQN, SPW and MQC sites in the middle and lower reaches, water quality was generally classified between Class III and Class V. The primary pollutants in these areas were COD, NH_4^+-N, and TP, but concentration of these pollutants have notably decreased in recent years. Taking the year 2023 as an example, only the concentration of at WZQN, SPW and MQC sites in the middle and lower reaches of the Fen River Basin exceeded the Class II limit of surface water ammonia nitrogen (0.5 $mg \cdot L^{-1}$), with 3, 2, and 2 instances of exceeding the limit, respectively.

The original time series data (**Table 1 and Table 2**) indicate significant improvements in water quality indicators at all seven monitoring stations between 2016 and 2023.Most of the time series passed the 95% confidence interval of Daniel significance trend test. Specifically, except for the SL station, COD concentrations at all other six stations showed significant downward trends with a 95% confidence level. Similarly, except for the LMS and HXC sites, NH_4^+-N concentration at the other five stations also showed significant downward trends. These trends were consistent with the results from the Daniel significance trend applied to the trend component of the original data, confirming a significant reduction in pollutant concentrations.

Seasonal variations in water quality were also evident. The concentrations of NH_4^+-N and DO were significantly higher during dry seasons compared to the wet seasons at all seven monitoring stations. In contrast, COD and TP concentrations were much higher during the wet seasons. The seasonal fluctuations in water quality are influenced by both natural and anthropogenic factors both natural and anthropogenic factors. Industrial, domestic, and agricultural non-point emissions have contributed to poorer water quality in certain areas. Additionally, the tributaries of the Fen River are

mainly seasonal rivers, characterized by flood events in the summer and water shortages during the dry season. During the dry season, the river's runoff mainly comes from wastewater discharged from domestic and industrial production along the way, resulting in higher concentrations of water pollutants, especially NH_4^+-N. Conversely, the strong erosion and high sediment content during the flood season contribute to COD concentrations.

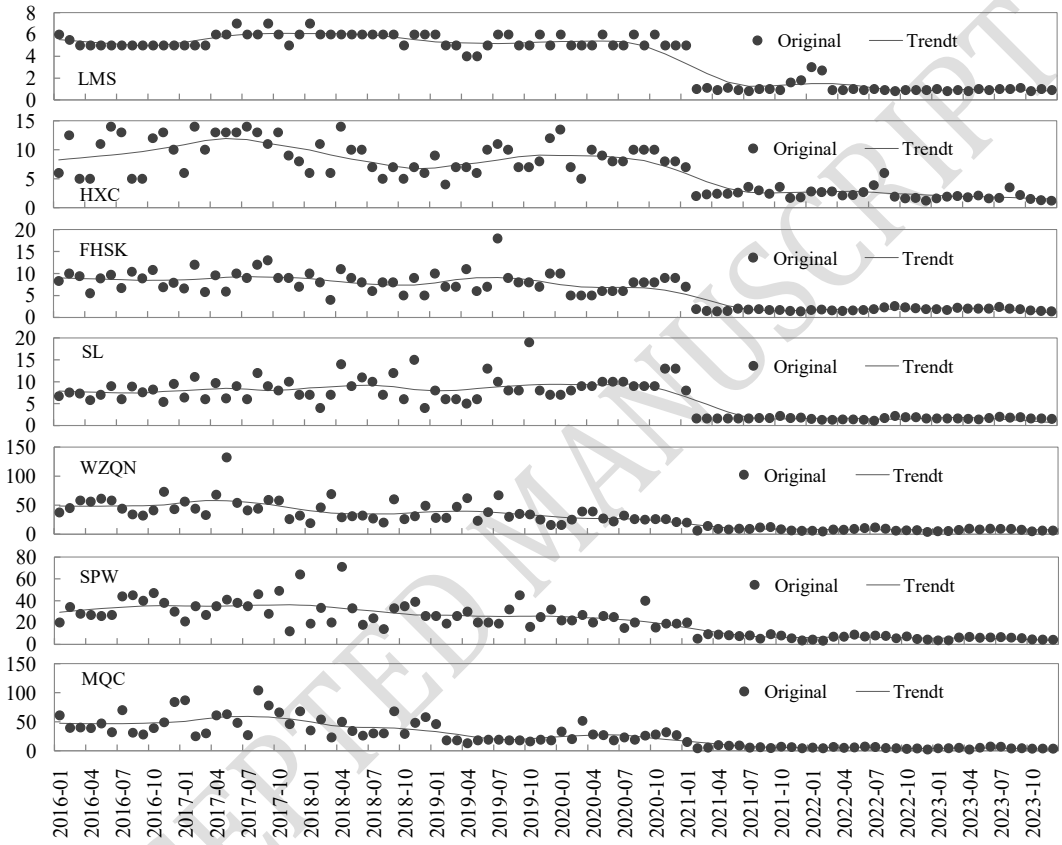

(a) COD

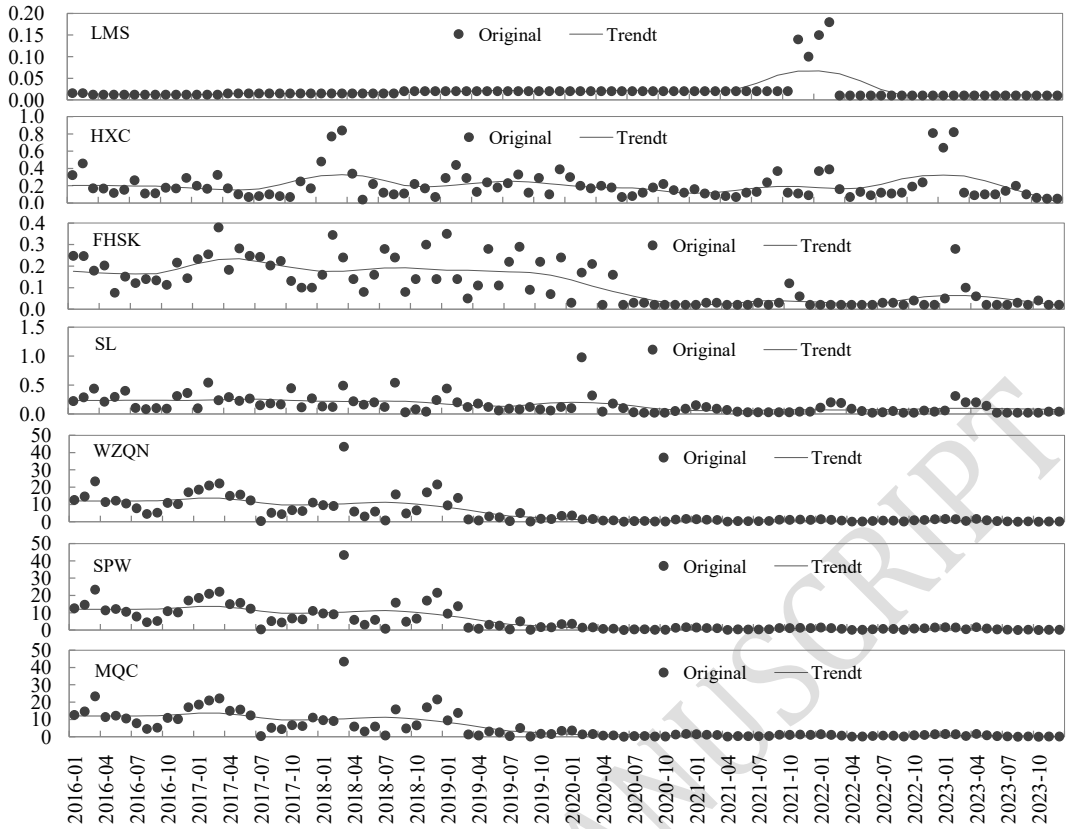

(b) NH_4^+-N

Fig.2 Temporal variations of main water quality parameters' concentrations in Fen river basin during 2016−2023

Table 1 The Daniel trend tests of the original COD and NH_4^+-N concentrations in Fen river basin during 2016−2023

Station	Period	n	Water quality index	$W_P(\alpha=0.05)$	$W_P(\alpha=0.01)$	r_S	Trend test
LMS	2016~2023	8	COD	0.707	0.834	-0.714	Significant decrease**
	2016~2023	8	NH_4^+-N	0.707	0.834	0.321	Not significant
HXC	2016~2023	8	COD	0.707	0.834	-0.881	Significant decrease***
	2016~2023	8	NH_4^+-N	0.707	0.834	0.024	Not significant
FHSK	2016~2023	8	COD	0.707	0.834	-0.857	Significant decrease***
	2016~2023	8	NH_4^+-N	0.707	0.834	-0.786	Significant decrease**
SL	2016~2023	8	COD	0.707	0.834	-0.524	Not significant
	2016~2023	8	NH_4^+-N	0.707	0.834	-0.857	Significant decrease***
WZQN	2016~2023	8	COD	0.707	0.834	-0.976	Significant decrease***
	2016~2023	8	NH_4^+-N	0.707	0.834	-0.905	Significant decrease***
SPW	2016~2023	8	COD	0.707	0.834	-0.976	Significant decrease***

Station	Period	n	Water quality index	$W_P(\alpha=0.05)$	$W_P(\alpha=0.01)$	r_S	Trend test
	2016~2023	8	NH_4^+-N	0.707	0.834	-0.976	Significant decrease***
MQC	2016~2023	8	COD	0.707	0.834	-0.952	Significant decrease***
	2016~2023	8	NH_4^+-N	0.707	0.834	-0.714	Significant decrease***
Mean	2016~2023	8	COD	0.707	0.834	0.976	Significant decrease***
	2016~2023	8	NH_4^+-N	0.707	0.834	0.905	Significant decrease***

Note:*, **, *** means passing the significance test of α=0.1, 0.05, 0.01 respectively.

Table 2 The Daniel trend tests of the trend components of COD and NH_4^+-N concentrations in Fen river basin during 2016−2023

Station	Period	n	Water quality index	$W_P(\alpha=0.05)$	$W_P(\alpha=0.01)$	r_S	Trend test
LMS	2016~2023	8	COD	0.707	0.834	-0.833	Significant decrease**
	2016~2023	8	NH_4^+-N	0.707	0.834	0.310	Not significant
HXC	2016~2023	8	COD	0.707	0.834	-0.881	Significant decrease***
	2016~2023	8	NH_4^+-N	0.707	0.834	-0.357	Not significant
FHSK	2016~2023	8	COD	0.707	0.834	-0.952	Significant decrease***
	2016~2023	8	NH_4^+-N	0.707	0.834	-0.833	Significant decrease**
SL	2016~2023	8	COD	0.707	0.834	-0.548	Not significant
	2016~2023	8	NH_4^+-N	0.707	0.834	-0.881	Significant decrease***
WZQN	2016~2023	8	COD	0.707	0.834	-0.952	Significant decrease***
	2016~2023	8	NH_4^+-N	0.707	0.834	-1.000	Significant decrease***
SPW	2016~2023	8	COD	0.707	0.834	-0.976	Significant decrease***
	2016~2023	8	NH_4^+-N	0.707	0.834	-0.905	Significant decrease***
MQC	2016~2023	8	COD	0.707	0.834	-0.952	Significant decrease***
	2016~2023	8	NH_4^+-N	0.707	0.834	-0.762	Significant decrease***
Mean	2016~2023	8	COD	0.707	0.834	-0.976	Significant decrease***
	2016~2023	8	NH_4^+-N	0.707	0.834	-0.976	Significant decrease***

Note:*, **, *** means passing the significance test of α=0.1, 0.05, 0.01 respectively.

Table 3 Statistics of water quality indexes in Fen river basin during wet and dry seasons in 2023 $mg \cdot L^{-1}$

Stations	Periods	COD	NH_4^+-N	TP	DO
Upstream stations	Wet season	2.1	0.05	0.045	6.4
	Dry season	1.5	0.14	0.016	9.8

Stations	Periods	COD	NH_4^+-N	TP	DO
	Difference	-0.6	0.09	-0.029	3.4
Three stations in the middle and downstream	Wet season	7.8	0.31	0.139	6.9
	Dry season	5.2	0.84	0.107	11.1
	Difference	-2.6	0.53	-0.033	4.2
Mean of seven stations	Wet season	4.3	0.15	0.082	6.6
	Dry season	3.5	0.51	0.065	10.5
	Difference	-0.9	0.36	-0.017	3.9

In recent years, significant improvements in the environmental quality of Fen River have been continuously observed, largely due to the implementation of water source protection and pollution control measures. In 2018, Shanxi Province issued the "Overall Plan for Ecological Protection and Restoration of the 'Seven Rivers' Basin" with a Focus on the Fen River. This was followed by the "Decision on Resolutely Winning the Battle of Fen River Basin Governance" in 2019, which has contributed to substantial reductions in industrial pollutants and improvements in water treatment rates. The goal of "a flood of clean water entering the Yellow River" has been largely achieved In January 2022, the Fen River Protection Regulations were enacted, providing clear provisions for water resource management, pollution prevention, and ecological restoration. Further, the "Ecological Protection and High-Quality Development Plan for the Yellow River Basin in Shanxi Province," was issued in April 2022 emphasized pollution control in the Fen River Basin and promoted targeted, scientific, and regulatory governance. According to the Statistical Yearbook of Urban and Rural Construction in 2022, as the end of 2022, the processing capacity of sewage treatment plants in China had reached 216 million cubic meters per day, with an urban sewage treatment rate of 98.11% and a centralized collection rate of 70.1% for urban domestic sewage. In Shanxi Province, sewage treatment capacity was 3.67 million cubic meters per day, with a treatment rate of 98.48% and a collection rate of 71.1%, both surpassing the national averages (Shanxi Provincial Department of Water Resources, 2023). Above all, these measures have greatly reduced the discharge of wastewater pollutants and contributed to the improved water quality in the Fen River basin.

3.2 Spatial variation of water quality

The spatial distribution of water quality in the Fen River Basin from 2016 to

2023 (presented in **Fig.3**) demonstrated notable variations between the upstream and downstream regions. Water quality in the middle and lower reaches fluctuated between III and V levels, while the upstream areas consistently maintained higher water quality levels, classified as Class I and II. During this period, the proportion of Class I-III water sections in the Basin ranged from 24.0% to 68.8%, whereas the proportion of worse-than-Class V sections varied between 0% and 72.7%. A significant upward trend was observed in proportion of water quality sections in Class I-III (rs=0.415, α=0.05), with a monthly increase of 0.2 percentage points. Conversely, the proportion of Class V water sections showed a significant downward trend, (rs=-0.803, α=0.05), decreasing by 0.9 percentage points per month. Although substantial progress has been made in eliminating many poor water quality sections with Class V, the water quality in certain middle and lower reaches, such as the WZQN station, remains poor, particularly during dry seasons in recent years. Spatial clustering analysis of COD concentration divided the seven monitoring sites into two categories: LMS, HXC, FHSK and SL formed the first category, while WZQN, SPW and MQC constituted the second. For the NH_4^+-N concentration, the sites were classified into three categories: LMS, HXC, FHSK and SL comprised the first category, WZQN formed the second category, and SPW and MQC constituted the third. The spatial clustering results aligned with the geographical location zoning of the seven sites. Given its location and severe pollution levels, WZQN station was selected as a representative site for focused analysis in the middle and lower reaches.

The spatial influencing factors of water quality can be summarized into two categories: natural factors and human activities. This study initially selected precipitation and surface water resources as the natural factors, while the human activities factors selected population, GDP, and pollutant emissions in wastewater. Grey correlation analysis (as shown in Table 4) revealed that population density was the predominant factor in the middle and lower reaches, with wastewater emission having the most significant impact on water quality. Gu et al. (2020) pointed out that large-scale domestic sewage discharges and emissions from heavy chemical industry as the primary contributors to severe pollution at WZQN station. According to the Water Resources Bulletin of Shanxi Province, total wastewater discharge in 2017 amounted to 788 million tons, with 25.2% originating from industrial sources. The Fen River received 336 million tons of wastewater, accounting for 42.6% of the

province's total wastewater discharge (Shanxi Provincial Department of Water Resources, 2018). By 2022, total wastewater discharge in Shanxi Province had risen to 1.097 billion tons, with industrial contributions increasing to 41.3% (Shanxi Provincial Department of Water Resources, 2023). Furthermore, data from the Shanxi Provincial Statistical Yearbook data revealed that in 2019, total COD and NH_4^+-N emissions were 109,200 tons and 11,200 tons, respectively, with domestic sources accounting for 62.5% and 87.8% of these pollutants (Shanxi Provincial Bureau of Statistics, 2023). These findings indicate a marked increase in the impact of domestic sewage on the Fen River Basin, while industrial emissions have proportionally decreased. The large volume of pollutants discharged—exceeding the river's self-purification capacity—remains the fundamental cause of the persistent and severe water pollution observed in the middle and lower reaches of the Fen River.

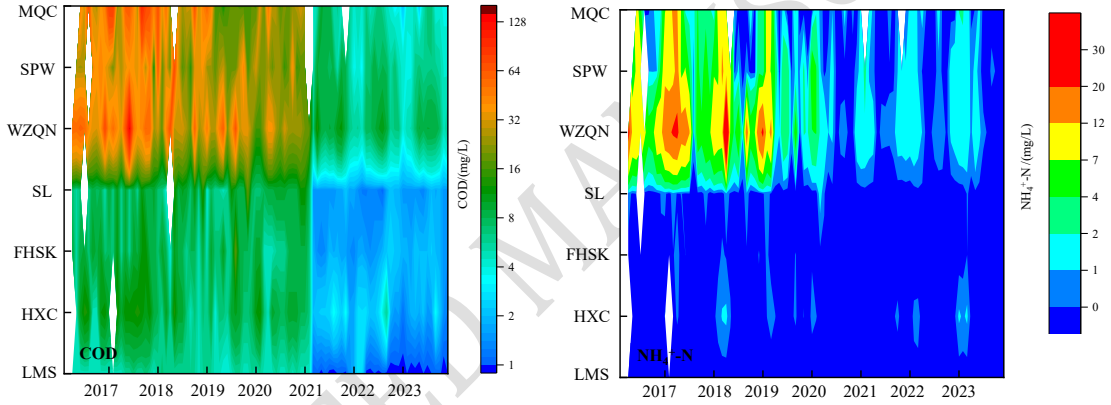

(a) Interpolated distribution

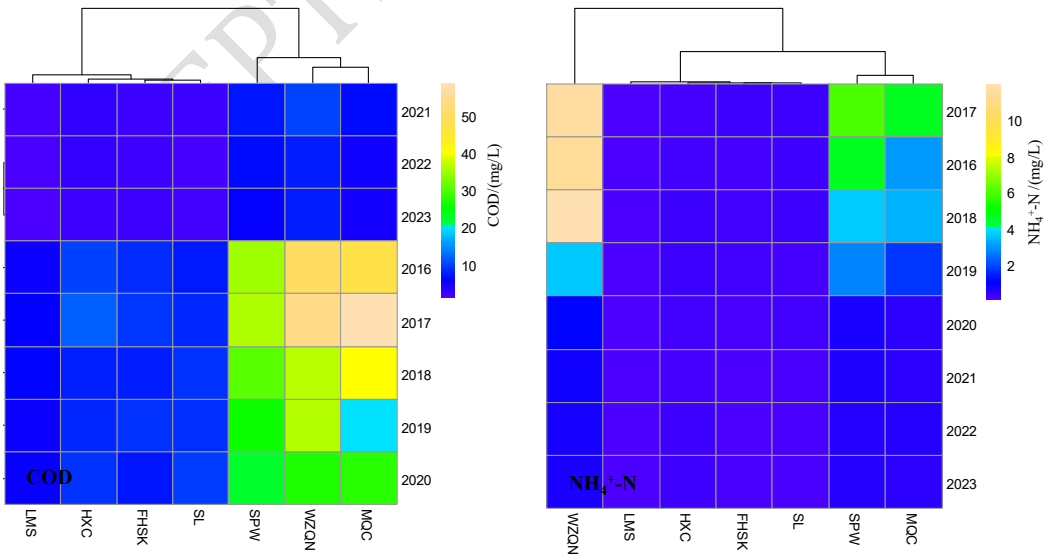

(b) Cluster distribution

Fig.3 Cluster distribution of water quality in seven monitoring sections of the Fen River Basin from 2016 to 2023

Table 4. Grey correlation degree between water indexes and social driving factors, hydrometeorological factors in Fen river basin

City	Station	WQI	GDP	Population	Rainfall	SWR	COD emissions	NH_4^+-N emissions
Xinzhou	LMS	COD	0.7676	0.8341*	0.8148	0.8290	0.5094	0.7786
		NH_4^+-N	0.8260*	0.7291	0.6883	0.7186	0.5802	0.7045
Xinzhou	HXC	COD	0.7800	0.8317*	0.8114	0.7668	0.5051	0.7767
		NH_4^+-N	0.7090	0.7511	0.7388	0.8009*	0.4761	0.6973
Taiyuan	FHSK	COD	0.7627	0.8183*	0.8177	0.6856	0.5020	0.7649
		NH_4^+-N	0.6554	0.7048*	0.6978	0.6004	0.4665	0.6817
Taiyuan	SL	COD	0.7801	0.8335*	0.7821	0.7437	0.5344	0.8214
		NH_4^+-N	0.7034	0.7576	0.7453	0.6883	0.4965	0.8092*
Jinzhong	WZQN	COD	0.7274	0.7821*	0.7224	0.7069	0.4851	0.7211
		NH_4^+-N	0.5785	0.6198	0.6501	0.6162	0.5054	0.6531*
Linfen	SPW	COD	0.7349	0.8037*	0.7183	0.6959	0.4944	0.7359
		NH_4^+-N	0.6720	0.6994	0.6689	0.6403	0.4933	0.7263*
Yuncheng	MQC	COD	0.7339	0.7996*	0.7608	0.7366	0.5856	0.7689
		NH_4^+-N	0.6532	0.7100	0.6784	0.6364	0.5217	0.7059*

Note:* means the largest GRD.

3.3 Impact of the COVID-19 Lockdown on Water Quality

On December 31, 2019, the Chinese government reported the first case of COVID-19 in Wuhan, Hubei Province (Kang et al., 2020). In response to the pandemic, Wuhan implemented strict measures in January 2020 to curb the virus's spread, including self-isolation, social distancing measures, traffic restrictions, and community controls (Deng and Peng, 2020), followed closely by other major cities in China (Le et al., 2020). Wuhan was the last city to reopened in April 2020, and after that only a few provinces and cities experienced sporadic outbreaks. In March 2022, China faced another sustained epidemic that lasted for about three months, until May 2022 (Meng and Zhang, 2023). During the first lockdown, industries came to a halt, commercial institutions were largely closed, and transportation systems were nearly at a standstill. The second wave of the epidemic, which affected only certain provinces and cities, did not lead to a nationwide large-scale lockdown, and is referred to as the "semi-lockdown period." If the water quality was improved during the semi lockdown

period, let alone during the full lockdown period. This study selected second epidemic period and defined the research period as follows:

- Pre-lockdown period: December 2021 to January 2022 (3 months);
- Lockdown period (second epidemic): March to May 2022 (3 months);
- Post-lockdown period: June to August 2022 (3 months).

Year-on-year comparison data (shown in **Fig.4**) reveals that during the lockdown period in 2022, concentrations of key water pollutants were significantly lower compared to the same period in 2021 and 2023. Specifically: COD concentration during the lockdown was 8.0 mg/L, 24.5% lower than in 2021 and 4.6% lower than in 2023. NH_4^+-N concentration was 0.42 mg/L, a 32.9% decrease from 2021 and 60.0% from 2023. TP concentration was 0.153 mg/L, 32.0% lower than in 2021 and 25.9% lower than in 2023. Turbidity during the lockdown period was 93.8 NTU, showing a 29.1% decrease from 2021 and 61.1% from 2023. These results indicate that the epidemic control measures from March to May 2022 significantly reduced pollutants concentrations, improving water transparency.

In the month-to-month analysis (shown in **Fig.5**), the following trends were observed: COD concentration was 115.8% higher during the lockdown period compared to the Pre-lockdown period, but 24.1% lower than in the post-lockdown period. NH_4^+-N concentration was 39.8% lower than the pre-lockdown period and 40.5% lower than the post-lockdown period. TP concentration was 73.8% higher than in the pre-lockdown period but 19.9% lower than in the post-lockdown periods. Turbidity was 26.2% lower than in the pre-lockdown period and 45.1% lower than in the post-lockdown periods. These month-to-month variations highlight that the water quality changes during the lockdown period were not consistent, which may be attributed to the seasonal variation in water quality caused by factors such as flood and dry seasons.

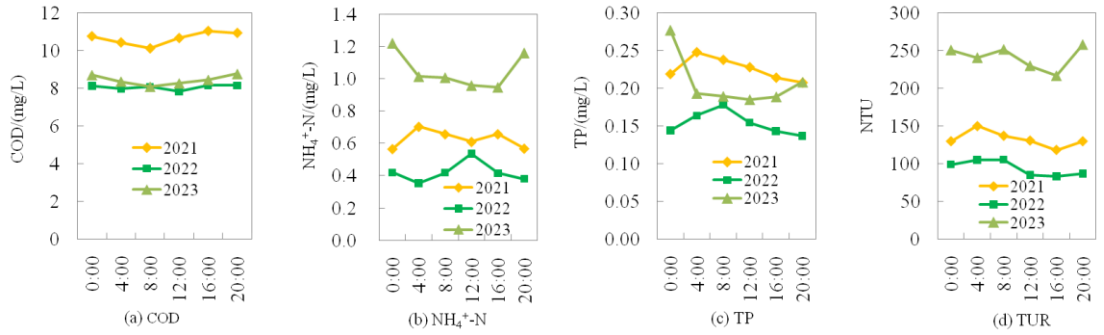

Fig.4 Variations in water quality indicators at WZQN station in the Fen River Basin from March to May, 2021−2023

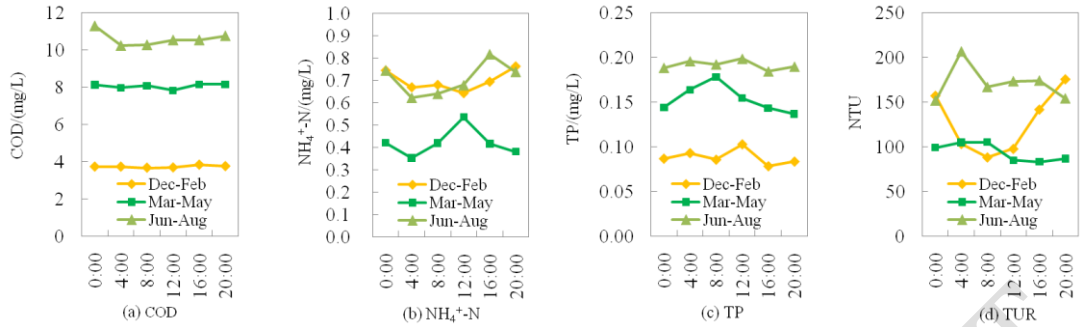

Fig.5 Variations in water quality indicators at WZQN station in the Fen River Basin before and after the epidemic period in 2023

3.4 Water Quality Simulation and Prediction

This research further selected the WZQN Station, located in the heavily polluted middle and lower reaches of the Fen River Basin, for water quality prediction and analysis (as shown in **Fig.6**). This study set the sequence from 2016 to 2022 as the model training dataset and the sequence in 2023 as the model validation dataset. The correlation coefficients between the predicted and observed values for COD and NH_4^+-N were 0.73 and 0.81, respectively, indicating a strong model fit. Additionally, the standardized mean deviations for COD and NH_4^+-N were 0.26 and 0.07, respectively, further confirming the good predictive performance of the LSTM model. The simulated results of the LSTM are better and meet the requirements of simulation accuracy. It showed that the LSTM showed high potential in future water environment monitoring and supervision, while the higher R^2 scores of 0.82 were achieved for TN prediction (Gao et al., 2024). The model predicted that the averaged COD and NH_4^+-N concentrations at WZQN station from 2024 to 2025 would be 5.0 ± 2.7mg/L and 0.42 ± 0.33 mg/L, respectively. By 2025, the COD concentration is expected to stabilize below the threshold set by the Surface Water Environmental Quality Standard (GB 3838—2002) for Class II (COD ≤ 15 mg/L) water quality. However, while the NH_4^+-N concentration is predicted to meet the water quality standard (NH_4^+-N ≤ 0.5 mg/L), it is expected to exceed this limit during the dry season of 2025. Therefore, further attention should be given to the seasonal variations in NH_4^+-N concentrations to ensure long-term compliance with water quality standards.

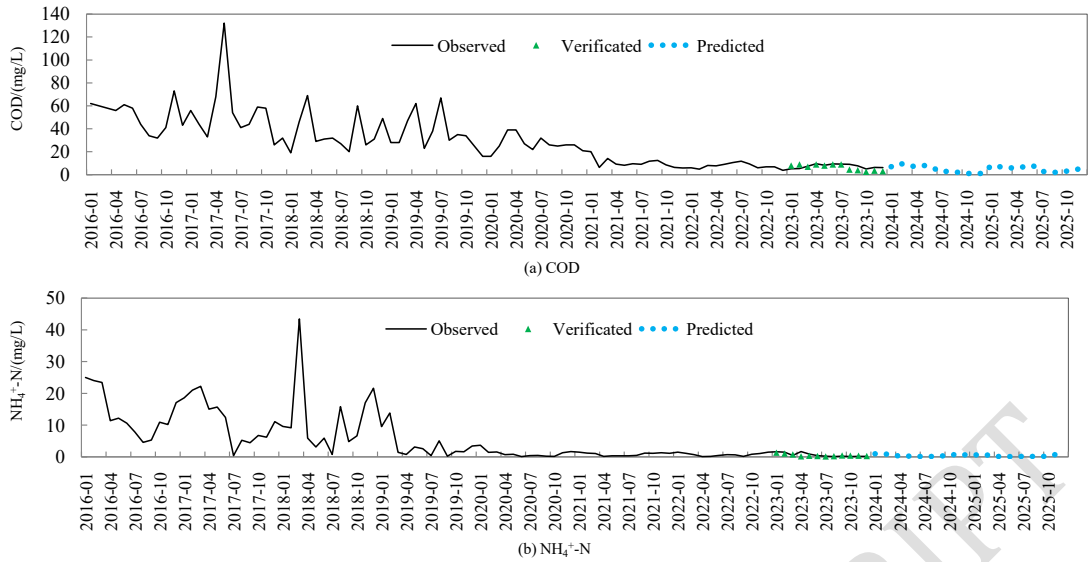

Fig.6 Prediction of COD and NH_4^+-N concentrations at WZQN station based on the LSTM method

4 Conclusions

The research systematically analyzed the water quality evolution trends and influencing factors in Fen River Basin by comprehensively applying statistical analysis methods such as Daniel trend test, Seasonal and Trend decomposition using Loess, grey correlation and Long Short-Term Memory neural network. From 2016 to 2023, the Fen River's water quality improved significantly, shifting from severe pollution to mild pollution. Upstream areas generally exhibited Class I–II water quality under GB 3838—2002 standards, while middle and lower reaches, although still relatively poor, showed notable elimination of inferior Class V water sections. COD and NH_4^+-N were identified as primary pollutants.

Although middle and lower reaches demonstrated significant improvement trends in key water quality indicators, NH_4^+-N concentrations at some upstream stations showed limited reduction. The improvements in the Fen River's environmental quality can largely be attributed to the implementation of water source protection and pollution control measures in recent years. It is noteworthy that the significant reduction in water usage for industrial, agricultural, and domestic purposes during the COVID-19 lockdown markedly improved water quality. This underscores the potential of targeted reductions in human activity to improve water quality. However, we projections for the end of the 14th Five-Year Plan indicate that NH_4^+-N concentrations may still exceed the Class II surface water quality standard (GB

3838—2002) limit (0.5 mg/L) during dry seasons, necessitating continued focus on controlling domestic pollution. Otherwise, the COD and TP concentrations were much higher during the wet seasons. Therefore, we should pay close attention to the changes in water quality during this period and carry out scientific treatment of non-point source pollution in the future. Moreover, it is suggested that on the basis of doing a good job in water quality monitoring during this period, efforts should be focused on promoting the comprehensive treatment of non-point source pollution to promote the stable improvement of the river water environment.

Acknowledgements: This work was supported by the Fundamental Research Funds for the Central Universities (3142023017, 3142021002, 3142023021), the Langfang science and technology support plan project (2024013020, 2024013033, 2023013101) and the Fundamental Research Funds for the Central Public-interest Scientific Institution (grant number 2024YSKY-16).

Author Contributions

Linlin Li and Bingfen Cheng designed the study, performed data analysis and wrote the manuscript. Other coauthors contributed to the research design, proofreading and revision.

Additional Information

Competing Interests: The authors declare no competing interests.

References

Arif M, Kumar R, Parveen S J, 2020. Reduction in Water Pollution in Yamuna River Due to Lockdown under COVID-19 Pandemic. https://doi.org/10.26434/chemrxiv.12440525.

Chen, X., Strokal, M., Van Vliet, M. T. H., et al., 2019. Multi-scale modeling of nutrient pollution in the rivers of China. *Environmental Science & Technology*, 53(16), 9614–9625. https://doi.org/10.1021/acs.est.8b07352.

Cheng, B. F., Xia, R., Zhang, Y., et al., 2019. Characterization and causes analysis for algae blooms in large river systems. *Sustainable Cities and Society*, 51, 101707. https://doi.org/10.1016/j.scs.2019.101707.

Cleveland, W. S. (1979). Robust locally weighted regression and smoothing scatter plots. *Journal of the American Statistical Association*, 74(368), 829–836. https://doi.org/10.1080/01621459.1979.10481038.

Cleveland, W. S., & Devlin, S. J. (1988). Locally weighted regression: An approach to regression

analysis by local fitting. *Journal of the American Statistical Association*, 83(403), 596–610. https://doi.org/10.1080/01621459.1988.10478639.

Daniel, W. W., 1990. Spearman rank correlation coefficient. In *Applied Nonparametric Statistics* (2nd ed., pp. 358–365). Boston: PWS-Kent.

Deng, J. L., 1985. *The grey control system*. Wuhan: Huazhong University of Science and Technology Press.

Deng, S., & Peng, H., 2020. Characteristics of and public health responses to the coronavirus disease 2019 outbreak in China. *Journal of Clinical Medicine*, 9, 575. https://doi.org/10.3390/jcm9020575.

Gao Z, Chen J, Wang G, et al., 2023. A novel multivariate time series prediction of crucial water quality parameters with Long Short-Term Memory (LSTM) networks. *Journal of Contaminant Hydrology*, 259,104262. https://doi.org/10.1016/j.jconhyd.2023.104262

Gers, F. A., Schraudolph, N. N., Schmidhuber, J., et al., 2003. Learning precise timing with LSTM recurrent networks. *Journal of Machine Learning Research*, 3, 115–143.

Grill, G., Lehner, B., Thieme, M., et al., 2019. Mapping the world's free-flowing rivers. *Nature*, 569(7755), 215–221. https://doi.org/10.1038/s41586-019-1111-9.

Gu, J., Zhang, X. M., Liu, M., et al., 2020. Variation of water environment quality in Fen River Basin from 2017 to 2019. *Shanxi Agricultural Economy*, 19, 64–70.

Hochreiter, S., & Schmidhuber, J., 1997. Long short-term memory. *Neural Computation*, 9(8), 1735–1780. https://doi.org/10.1162/neco.1997.9.8.1735.

Huang, J. H., Zhang, Y. J., Bing, H. J., et al., 2021. Characterizing river water quality in China: Recent progress and ongoing challenges. *Water Research*, 201, 117309. https://doi.org/10.1016/j.watres.2021.117309.

Kang, D., Choi, H., Kim, J., et al., 2020. Spatial epidemic dynamics of the COVID-19 outbreak in China. *International Journal of Infectious Diseases*, 94, 96–102. https://doi.org/10.1016/j.ijid.2020.03.067.

Le, T., Wang, Y., Liu, L., et al., 2020. Unexpected air pollution with marked emission reductions during the COVID-19 outbreak in China. *Science*, 369(6504), 702–706. https://doi.org/10.1126/science.abb7431.

Liu, D., Yang, H., Thompson, J. L. R., et al., 2022. COVID-19 lockdown improved river water quality in China. *Science of the Total Environment*, 802, 149585. https://doi.org/10.1016/j.scitotenv.2021.149585.

Meng, X. B., & Zhang, J., 2023. Impact of COVID-19 lockdown on water quality in China during

2020 and 2022: Two case surges. *Environmental Science and Pollution Research*, 30, 79386–79401. https://doi.org/10.1007/s11356-023-26299-9.

Ministry of Ecology and Environment, P. R. C., 2023. *Annual bulletin of China's ecology and environment in 2022*. Beijing: Ministry of Ecology and Environment, P. R. C. Retrieved from http://www.cnemc.cn/jcbg/zghjzkgb/.

Saadat, S., Rawtani, D., & Hussain, C. M., 2020. Environmental perspective of COVID-19. *Science of the Total Environment*, 728, 138870. https://doi.org/10.1016/j.scitotenv.2020.138870.

Shanxi Provincial Bureau of Statistics, 2023. *Shanxi Statistical Yearbook 2022*. Beijing: China Statistics Press. Retrieved from http://tjj.shanxi.gov.cn/tjsj/tjnj/nj2023/zk/indexch.htm.

Shanxi Provincial Department of Water Resources, 2018. *Water resources bulletin of Shanxi Province in 2017*. Taiyuan: Shanxi Provincial Department of Water Resources.

Shanxi Provincial Department of Water Resources, 2023. *Water resources bulletin of Shanxi Province in 2022*. Taiyuan: Shanxi Provincial Department of Water Resources.

Silawan, T., Singhasivanon, P., Kaewkungwal, J., et al., 2008. Temporal patterns and forecast of dengue infection in Northeastern Thailand. *Southeast Asian Journal of Tropical Medicine and Public Health*, 39(1), 90-98.

Spearman C,1904. The proof and measurement of association between two things. *Journal of Applied Psychology*, 15(1): 72-101.

Suresh M, Surendran R, Raveena S, et al., 2025. Wastewater recycling integration with lot sensor vision for real-time monitoring and transforming polluted ponds into clean ponds using HG-RNN. Global NEST Journal, 27(4). https://doi.org/10.30955/gnj.06758

Tao, T., & Xin, K, 2014. A sustainable plan for China's drinking water: Tackling pollution and using different grades of water for different tasks is more efficient than making all water potable. *Nature*, 511(7511), 527–529. https://doi.org/10.1038/511527a.

Venkatraman, M., Surendran R, Senduru S, et al., 2025. Water quality prediction and classification using Attention based Deep Differential RecurFlowNet with Logistic Giant Armadillo Optimization, Global NEST Journal, Accept. https://doi.org/10.30955/gnj.0679.

Xia, R., Wang, G. S., Zhang, Y., et al., 2020. River algal blooms are well predicted by antecedent environmental conditions. *Water Research*, 185, 116221. https://doi.org/10.1016/j.watres.2020.116221.

529 Zhang, Q. Q., Ying, G. G., Pan, C. G., et al., 2015. Comprehensive evaluation of antibiotics
530 emission and fate in the river basins of China: Source analysis, multimedia modeling, and
531 linkage to bacterial resistance. *Environmental Science & Technology*, 49(11), 6772–6782.
532 https://doi.org/10.1021/acs.est.5b01026.
533 Zhang, B. F., Chen, F., Tian, X. Q., et al., 2020. Research on water quality variation of seven
534 major water systems in China from 2005 to 2017. *Yangtze River*, 51(7), 33–40.
535 Zhai, X. Y., Xia, J., & Zhang, Y. Y., 2014. Water quality variation in the highly disturbed Huai
536 River Basin, China, from 1994 to 2005 by multi-statistical analyses. *Science of the Total*
537 *Environment*, 496, 594–606. https://doi.org/10.1016/j.scitotenv.2014.07.005.